Systematic Variation of Resistant Cells to Identify Asymptomatic Disease Thresholds in Influenza A Virus Infection

Melissa Terry

MCDB 172
University of California, Santa Barbara
23 March 2023

Abstract

This study utilizes a dynamical model of the human immune response to influenza A virus infection developed by *Hancioglu et al.* to investigate how variation in immune response affects disease severity. The study aims to determine the level of cellular resistance at which disease becomes asymptomatic by systematically varying the level of resistant cells and analyzing the resulting disease outcomes using Python simulations. The goal of the study is to provide insight into the immune mechanisms that underlie disease progression and identify potential targets for intervention, particularly in the design and implementation of effective vaccination strategies. By exploring the complex dynamics of the host-pathogen interaction, this approach can be applied to a range of infectious diseases, offering a powerful tool for understanding disease transmission and control.

---

1. Introduction

Influenza A virus—of the family *Orthomyxoviridae*—continues to present a substantial threat to public health, causing seasonal epidemics that result in over 650,000 deaths per year (Lee & Ryu, 2021). Influenza A virus (IAV) is a single stranded, negative sense RNA virus—class V of the Baltimore classification system. IAV is of particular interest, as it is known to undergo antigenic shifts and drifts, where its surface glycoproteins, hemagglutinin, and neuraminidase undergo periodic mutations (Moghadami, 2016). This constant antigenic evolution is due to the segmented nature of its genome, which makes it highly susceptible to genetic reassortment and allows the virus to evade host immune responses. Such genetic reassortment additionally enables animal and human strains to converge and circulate, resulting in intermittent pandemics causing disruption at a global level (Hancioglu et al., 2007). The significant variation in IAV strains from one season to another has made it difficult to develop effective strategies for prevention and control. To address this issue, it is essential to understand the complex dynamics between the virus and the human immune response.

In recent years, mathematical models have become indispensable in studying the dynamics of disease transmission at both the cellular and population levels. At the cellular level, such models allow for the prediction of disease severity and the efficacy of interventions. Among these models, dynamical systems provide a means of investigating the complex mechanisms that underpin biological function. That is, in capturing the temporal changes in the cellular immune response, these models offer insight into the potential impact of intervention—facilitating development of strategies for disease control and damage reduction. This study utilizes a system of ordinary differential equations which together model the human immune response to IAV infection. In reproducing and expanding upon a model by *Hancioglu et al.*, this study attempts to elucidate the factors most important in disease reduction. The immune response to viral infection is complex, and it is important to note that the modulation of resistant cells presented here do not wholly encompass the complexity of the human immune system and may not reflect the full range of immunological responses. Nonetheless, the model provides a useful framework for exploring how variation in immune response affects disease outcomes and identifying potential targets for intervention. Further experimentation presented in this study aims to shift focus to effectiveness of intervention, and thresholds necessary for reduced expression of disease.

2. Methods & Results

2.1 Dynamical Model and Variables

The simulations presented in this paper utilize a system of 10 ordinary differential equations from *Hancioglu et al.*, which represents the adaptive and innate immune response to infection via the influenza A virus (IAV). The intent of the model presented in this paper is to simulate a system that has had exposure to a similar IAV strain through vaccination, prior to infection. In order to do so, the model was first run under standard conditions (e.g. a healthy, unvaccinated host that has not been exposed to IAV on day zero) to ensure that the system of equations accurately reflects the course of infection.

Table 1 Variable Descriptions from *Hancioglu et al.*

Variable	Description
V	Viral load per epithelial cell
H	Proportion of healthy cells
I	Proportion of infected cells
M	Activated antigen presenting cells per homeostatic level
F	Interferons per homeostatic level of macrophages
R	Proportion of resistant cells
E	Effector cells per homeostatic level
P	Plasma cells per homeostatic level
A	Antibodies per homeostatic level
S	Antigenic distance

In the following system, V corresponds to the overall concentration of the virus per epithelial cell, and under standard conditions is assumed to be 0.01. Variable H serves to indicate the proportion of healthy cells in the system, and has an initial value of 1 (e.g. 100% of cells are healthy). Healthy cells are defined here as cells that are neither infected nor resistant to the virus. Conversely, infected cells I are those that have been exposed to the virus, and therefore have an initial value of zero. M, F, and R represent cells that have some immunological response to viral exposure, and are therefore also set to zero under standard conditions. Immunological systems in place prior to viral exposure are represented by E, P, and A, with initial values of 1 under standard conditions. Antigenic distance, represented by S, is predicted to be 0.1 under standard conditions, assuming exposure to previous IAV strains. Of particular interest in this experiment are variables H, M, F, and R, as modulations of these variables away from standard conditions allow for the simulation of infection in a host that has been vaccinated. The system of equations is formulated as follows, and represents the rate of change per variable during viral infection:

(1) $dVdt = \gamma_V I - \gamma_{VA} SAV - \gamma_{VH} HV - \alpha_V V - \frac{a_{V1} V}{1 + a_{V2} V}$

(2) $dHdt = (b_{HD} D(H+R)) + (a_R R) - (\gamma_{HV} VH) - (b_{HF} FH)$

(3) $dIdt = (\gamma_{HV} VH) - (b_{IE} EI) - (a_I I)$

(4) $dMdt = (((b_{MD} D) + (b_{MV} V)) * (1 - M)) - (a_M M)$

(5) $dFdt = (b_F M) + (c_F I) - (b_{FH} HF) - (a_F F)$

(6) $dRdt = (b_{HF} FH) - (a_R R)$

(7) $dEdt = (b_{EM} ME) - (b_{EI} IE) + (a_E (1 - E))$

(8) $dPdt = (b_{PM} MP) + (a_P (1 - P))$

(9) $dAdt = (b_A P) - (\gamma AVSAV) - (a_A A)$

(10) $dSdt = rP(1 - S)$

2.2 Parameters

All parameters for the dynamical system were estimated in *Hancioglu et al.*, and remain unchanged for the duration of this experiment. Under standard conditions, parameters for the system are as follows:

Table 2
Parameter Descriptions and Values for standard conditions from *Hancioglu et al.*

Parameter	Value	Description
γ_V	510	Rate constant of influenza A virus (IAV) particles secretion per infected epithelial cells
γ_{VA}	619.2	Rate constant of neutralization of IAV by antibodies
γ_{VH}	1.02	Rate constant of adsorption of IAV by infected epithelial cells
$alpha_V$	1.7	Rate constant of nonspecific IAV removal
a_{V1}	100	Rate constant of nonspecific IAV removal
a_{V2}	23000	Rate constant of nonspecific IAV removal
b_{HD}	4	Rate constant of regeneration of epithelial cells
a_R	1	Rate constant of epithelial cells' virus resistance state decay
γ_{HV}	0.34	Rate constant of epithelial cells infected by IAV
b_{HF}	0.01	Rate constant of epithelial cells' virus resistant state induction
b_{IE}	0.066	Rate constant of infected epithelial cells that CTL damage
a_I	1.5	Rate constant of infected epithelial cells damage by cytopathicity of IAV
b_{MD}	1	Rate constant of stimulation of antigen presenting cells by dead cells
b_{MV}	0.0037	Rate constant of stimulation of antigen presenting cells by virus particles
a_M	1	Rate constant of stimulated state loss of antigen presenting cells
b_F	250000	Interferon (IFN) production rate per APC
c_F	2000	Interferon (IFN) production rate per infected cell
b_{FH}	17	Rate constant of epithelial cells that IFN binds
a_F	8	Rate constant of IFN's natural decay
b_{EM}	8.8	Rate constant of stimulation of effector cells
b_{EI}	2.72	Rate constant of death of effectors by lytic interactions with infected epithelial cells
a_E	0.4	Rate constant of natural death of effector cells
b_{PM}	11.5	Rate constant of plasma cells production
a_P	0.4	Rate constant of natural death of plasma cells
b_A	0.043	Antibody production rate per plasma cells
γ_{AV}	146.2	Rate constant of antibodies which binds to IAV
a_A	0.043	Rate constant of natural death of antibodies
r	3e-5	Rate constant for S variable

2.3 Experimental Design and Results

All dynamical simulations presented in this paper are simulated using Python programming language, and depend on the scientific computing libraries Scipy ODEint for numerical integration, Numpy for data manipulation, as well as Matplotlib for graphical analysis.

The aim of this experiment is to examine how prior vaccination affects the progression of IAV infection. We first conducted the simulation under standard conditions, with a time course of 15 days and an interval of 1000 time points. Figure 1 illustrates the time courses of each variable, confirming that the simulation produces the anticipated course of IAV infection. Additionally, the figure displays the cumulative proportion of healthy, dead, infected, and resistant epithelial cell types, providing a comprehensive view of the infection's effects.

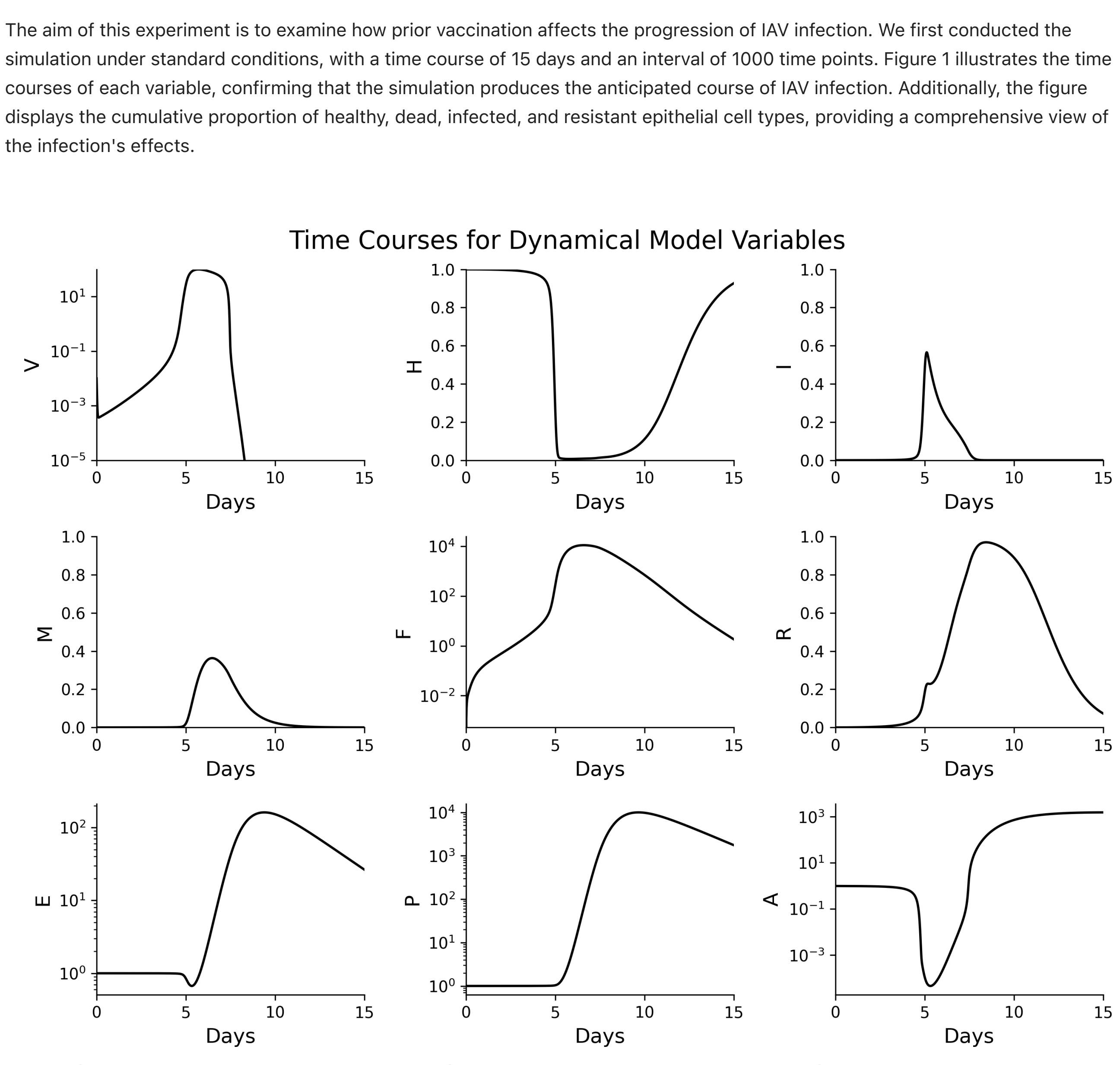

Figure 1. Time courses of the system variables under standard conditions, plotted over a 15-day time course with 1000 time points. To better illustrate the dynamics of the system, the variables V, F, E, P, and A are plotted on a linear x-axis and a logarithmic y-axis. The cumulative proportion of epithelial cell types is also shown at the bottom right, with healthy cells represented by the space above the blue curve, resistant cells between the blue and green curves, and infected cells between the green and red curves. Dead cells are represented by the area beneath the red curve. The simulation results confirm the anticipated course of IAV infection and provide a detailed overview of the infection's impact on different cell types.

In order to further establish the baseline for the system variables under standard conditions, the time courses for various levels of initial viral load were plotted. Figure 2a displays the time course of viral load for different V_o values ranging from 0.001 to 200, with V_1 = 0.00227 and V_2 = 0.1 representing the thresholds for typical disease and severe disease, respectively. In addition, Figure 2b illustrates the resulting cellular damage during the course of viral infection, while Figure 2c presents a phase diagram to depict the dependence on initial viral load. It should be noted figures 2a and 2c were plotted utilizing logarithmic scales for enhanced visual clarity.

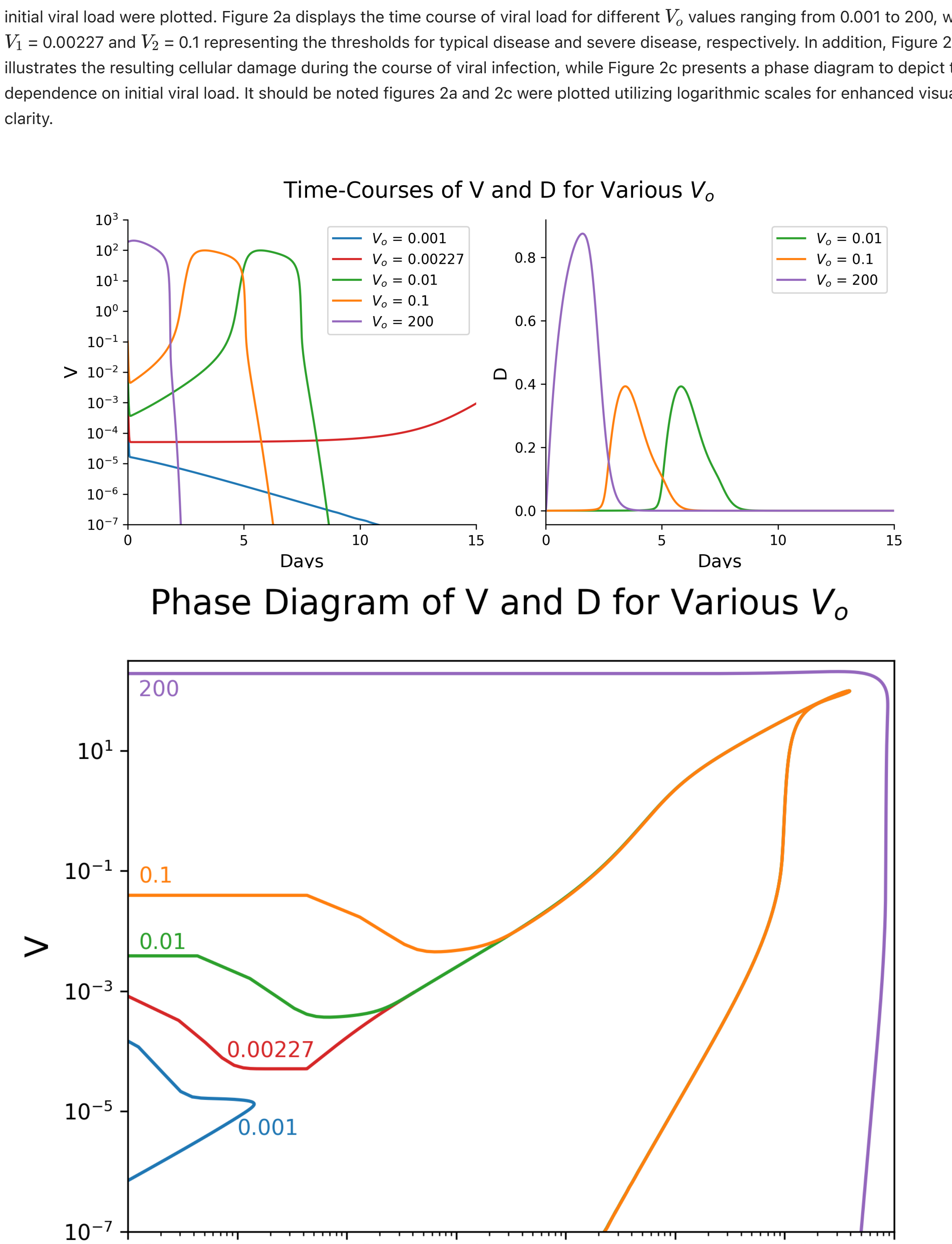

Figure 2. Time courses of viral load (a) and cellular damage (b) for V_o values ranging from 0.0010 to 200. (c) Phase diagram of log V vs log D, yielding a maximum viral load and maximum cell damage of $1.3x10^{10}$ particles per mL and 36%, respectively.

To simulate the conditions of vaccination, a time course of cellular damage under different initial antigenic distances was plotted. Antigenic distance indicates the compatibility between antibodies and the viral strain, with a value of 1 representing the highest affinity. The variable S_o represents the host's immune memory, and simulating its manipulation allows us to establish a baseline for further manipulation of initial values to simulate different vaccination levels.

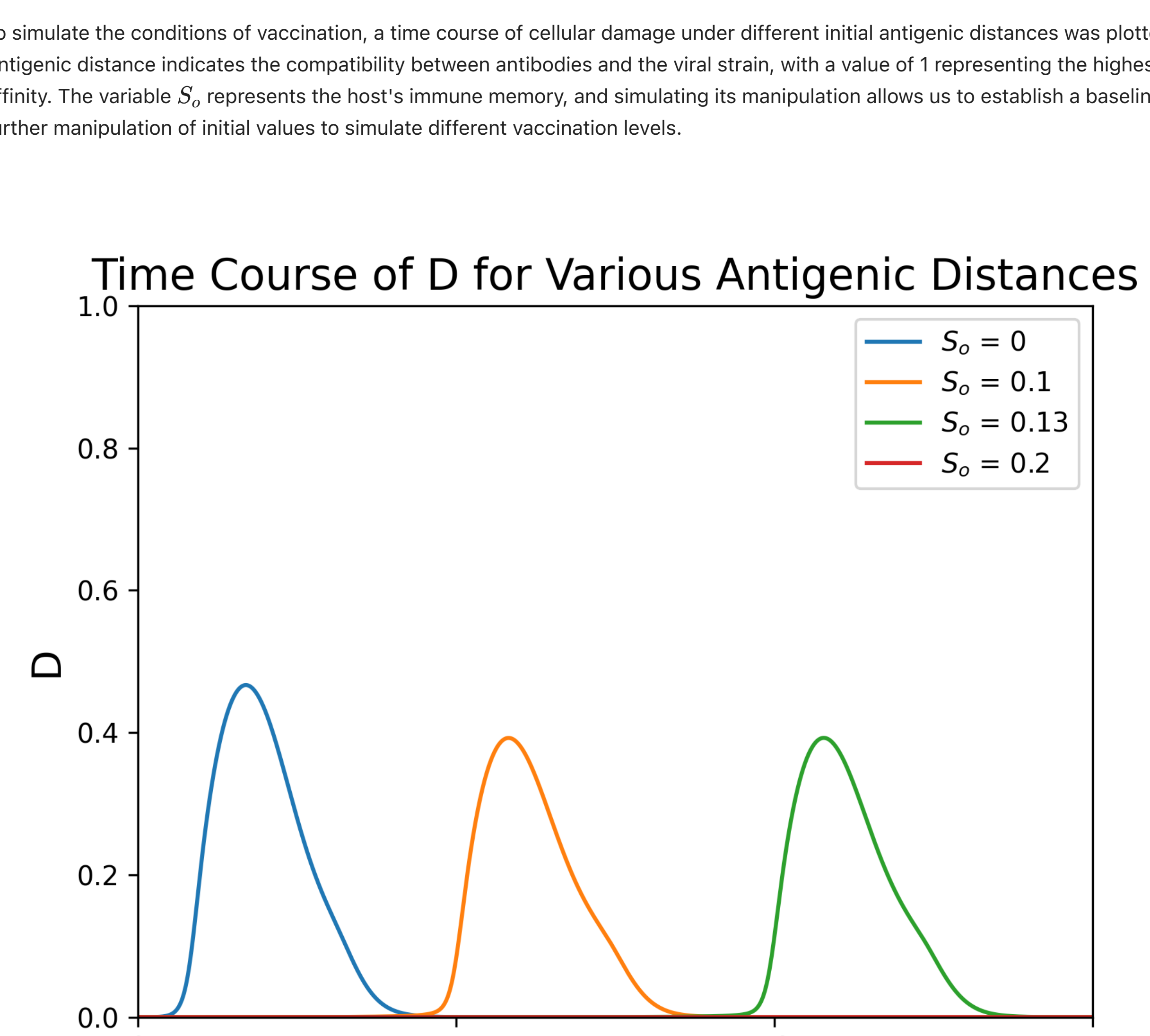

Figure 3. Time course of cellular damage for S_o values ranging from 0 to 0.2. The orange curve represents antigenic distance under standard conditions (mild compatibility), while manipulating its initial values results in delayed or expedited onset of cellular damage.

To further investigate the impact of vaccination on the course of disease, we plotted time courses of viral load and cellular damage with varied levels of resistant and healthy initial cell types. Figure 4a and b illustrates the impact of variation in resistant cells. As healthy cells and resistant cells are inversely proportional, a higher initial value for healthy cells (H) leads to a lower initial value for resistant cells (R), and vice versa.

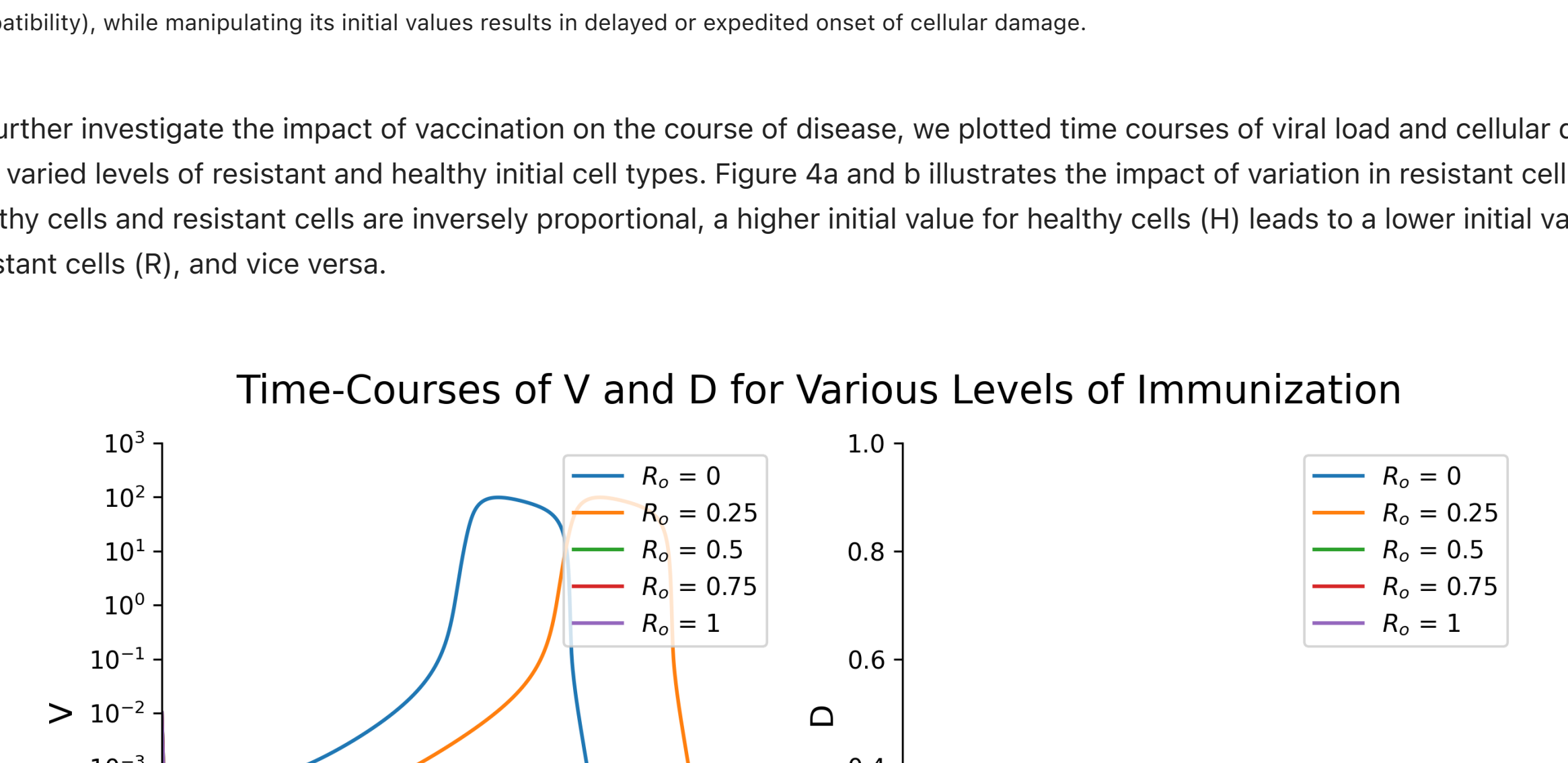

Figure 4. Time courses of viral load (a) and cellular damage (b) for R_o values ranging from 0 to 1. Note that disease becomes asymptomatic at an R_o value of 0.5.

Discussion

The results of this study offer valuable insights into the progression of influenza A infection (IAV) and the impact of various factors on disease severity, and enables the identification of critical conditions for vaccination efficacy. The computational model presented by *Hancioglu et al.* was successfully implemented, and the simulation accurately captured the expected course of IAV infection under standard conditions, as demonstrated in Figure 1. The fifth day of infection represented the peak of both viral load and cellular damage under standard conditions, setting a baseline for the simulation of vaccination.

Figure 2 serves as further confirmation of the model's implementation. The recreation of findings suggests that viral load per epithelial cell is a critical factor in determining the severity of cellular damage during IAV infection. The results demonstrate that cellular damage increases significantly with increased viral load, with damage peaked at 40% under standard conditions. The model was robust to variations in initial conditions, as cellular damage remained at 40% even with initial viral loads less than the maximum. The earlier onset of cellular damage with greater viral load confirms the intuitive understanding of the disease.

The impact of antigenic distance on disease progression was investigated in Figure 3, serving as the introduction to the impact of vaccination. Antigenic distance represents the affinity between the antibodies and the viral strain, with a value of 1 indicating the highest affinity. The results indicate that an absent antigenic distance (e.g. no recognition for the virus) increases cellular damage. However, for initial antigenic distances greater than zero, the higher the antigenic distance, the later the onset of cellular damage. The disease becomes asymptomatic at an antigenic distance of 0.2, suggesting the importance of the affinity of antibodies for the virus.

Figure 4 investigated the impact of varying levels of healthy and resistant initial cell types, simulating conditions of vaccination. The inverse proportionality between healthy and resistant cells was implemented, as the higher the initial value for healthy cells, the lower the initial value for resistant cells, and vice versa. The results suggest that a cellular resistance of 50% allows for asymptomatic disease expression, and resistance to the virus delays the onset of viral load.

These findings begin to investigate implications for the development of effective treatment and intervention measures for IAV infection. The results suggest that reducing the viral load per epithelial cell and increasing the affinity of antibodies for the virus can effectively reduce cellular damage and delay the onset of the disease. More importantly, the results also suggest that increasing the proportion of resistant cells can lead to asymptomatic disease expression.

One limitation of this study is the lack of variation of parameters. The assumption was made that manipulating initial values will have no impact on inherent disease mechanism rates, which will limit its generalizability to real-world situations.

Future directions for this research could include investigating the impact of other factors, such as the impact of both antigenic distance and cellular resistance to innate defense mechanisms. Further modifications should be made to the model to improve its accuracy and robustness to variations in initial conditions. In addition, the validation of the model using real-world data could strengthen the reliability of the findings.

In conclusion, the results of this study provide valuable insights into the factors that influence the severity and progression of IAV infection. The findings provide direction for the development of effective treatment and intervention measures for IAV infection and further investigation could yield executable results.

Works Cited

Hancioglu, B., Swigon, D., & Clermont, G. (2007). *A dynamical model of human immune response*

> *to influenza A virus infection*. Journal of Theoretical Biology, 246(1), 70–86.

Lee, S. J., & Ryu, J.-H. (2021). *Influenza viruses: Innate immunity and mrna vaccines*. Frontiers in

> Immunology, 12.

Moghadami, M. (2016). *A Narrative Review of Influenza: A Seasonal and Pandemic Disease*. Iranian

> Journal of Medical Sciences, 42, 2 - 13.